HHS Public Access

Author manuscript

Nanotoxicology. Author manuscript; available in PMC 2017 December 01.

Published in final edited form as:

Nanotoxicology. 2016 December ; 10(10): 1458–1468. doi:10.1080/17435390.2016.1235737.

Respiratory toxicity and immunotoxicity evaluations of microparticle and nanoparticle C60 fullerene aggregates in mice and rats following nose-only inhalation for 13 weeks

Brian C. Sayers[a,1], **Dori R. Germolec**[a], **Nigel J. Walker**[a], **Kelly A. Shipkowski**[a], **Matthew D. Stout**[a], **Mark F. Cesta**[a], **Joseph H. Roycroft**[a], **Kimber L. White Jr.**[b], **Gregory L. Baker**[c], **Jeffrey A. Dill**[c], and **Matthew J. Smith**[b,d]

[a]Division of the National Toxicology Program, National Institute of Environmental Health Sciences, 530 Davis Drive, Research Triangle Park, NC, USA

[b]Department of Pharmacology and Toxicology, Virginia Commonwealth University, 527 N. 12th Street, Room 2-009, Richmond, VA 23298, USA

[c]Battelle Toxicology Northwest, 900 Battelle Boulevard, Richland, WA 99354

[d]Richard Bland College of William & Mary, 8311 Halifax Road, McNeer Hall 127, Petersburg, VA 23805

Abstract

C60 fullerene (C60), or buckminsterfullerene, is a spherical arrangement of 60 carbon atoms, having a diameter of approximately 1 nm, and is produced naturally as a by-product of combustion. Due to its small size, C60 has attracted much attention for use in a variety of applications; however insufficient information is available regarding its toxicological effects. The effects on respiratory toxicity and immunotoxicity of C60 aggregates (50 nm [nano-C60] and 1 μm [micro-C60] diameter) were examined in B6C3F1/N mice and Wistar Han rats after nose-only inhalation for 13 weeks. Exposure concentrations were selected to allow for data evaluations using both mass-based and particle surface area-based exposure metrics. Nano-C60 exposure levels selected were 0.5 and 2 mg/m^3 (0.033 and 0.112 m^2/m^3), while micro-C60 exposures were 2, 15, and 30 mg/m^3 (0.011, 0.084, and 0.167 m^2/m^3). There were no systemic effects on innate, cell-mediated, or humoral immune function. Pulmonary inflammatory responses (histiocytic infiltration, macrophage pigmentation, chronic inflammation) were concentration-dependent and corresponded to increases in monocyte chemoattractant protein (MCP)-1 (rats) and macrophage inflammatory protein (MIP)-1α (mice) in bronchoalveolar lavage (BAL) fluid. Lung overload may have contributed to the pulmonary inflammatory responses observed following nano-C60 exposure at 2 mg/m^3 and micro-C60 exposure at 30 mg/m^3. Phenotype shifts in cells recovered from the BAL were also observed in all C60-exposed rats, regardless of the level of exposure. Overall, more severe pulmonary effects were observed for nano-C60 than for micro-C60 for mass-

[1]Correspondence: Brian C. Sayers, Ph.D., DuPont Haskell Global Centers for Health & Environmental Sciences, 1090 Elkton Rd, Newark, DE, USA, Tel (302) 366-5001, Brian.C.Sayers@dupont.com.

Declaration of Interest

This work was supported [in part] by the Intramural Research Program of the National Institutes of Health (NIH), National Institute of Environmental Health Sciences (NIEHS) and by NTP Contracts N01-ES-55538 and N01-ES-5553.

based exposure comparisons. However, for surface-area-based exposures, more severe pulmonary effects were observed for micro-C60 than for nano-C60, highlighting the importance of dosimetry when evaluating toxicity between nano- and microparticles.

Keywords

nanoparticles; immunotoxicity; inhalation; buckminsterfullerene; pulmonary inflammation

Introduction

Nanomaterials (NMs) are defined by the European Union (EU) as materials with at least one dimension between 1 nm and 100 nm (Bleeker et al. 2013; EU 2011). Although a definition has yet to be formally adopted by regulatory agencies in the United States (U.S.), the U.S. Food and Drug Administration (FDA) has recommended that the EU definition be used as a starting point for determining whether FDA-regulated products contain NMs (FDA 2011). C60 fullerene (C60), also known as buckminsterfullerene, is an arrangement of 60 carbon atoms in the shape of a truncated icosahedron (Kroto et al. 1985; Terrones and Mackay 1992). This NM has attracted much interest for a variety of potential uses, including medical, engineering, and electrical applications, due to its extremely small size. A single C60 particle has an estimated diameter of approximately 1 nm (Johnston et al. 2010; Kroto et al. 1985), and, as such, it is the smallest possible NM under the EU definition. However, like many other NMs, C60 can readily form aggregates of larger sizes.

Due to the significant interest in C60, and in light of the fact that C60 is produced naturally via combustion (Johnston et al. 2010), the potential toxicity of C60 exposure is an area of great concern (Balbus et al. 2007). The possible routes of human exposure to C60 include inhalation, oral, dermal, and parenteral (Johnston et al. 2010). It has been reported that oral C60 exposure has no associated toxicity, while intraperitoneal (*ip*) exposure to C60 can result in renal and hepatotoxicity (Johnston et al. 2010). In addition, *ip* exposure to C60 (60 mg/kg/day; 12 days) has been demonstrated to cause significant increases in both absolute and relative organ weight of the spleen, one of the primary immune organs (Chen et al 1998a).

Baker *et al.* (2008) evaluated pulmonary inflammatory effects in male rats following a ten-day nose-only inhalation exposure to C60 nano- and microparticles. No differences in bronchoalveolar lavage (BAL) fluid cell numbers were observed for alveolar macrophages, neutrophils or lymphocytes, however, BAL fluid protein concentration was increased following C60 nanoparticle exposure. BAL fluid cytokines TNF-α and IL-1β were increased in rats exposed to C60 microparticles. Pulmonary inflammatory effects, including increased numbers of neutrophils and levels of pro-inflammatory cytokines, have been previously reported in mice following intratracheal (*it*) instillation of C60 (Johnston et al. 2010; Park et al. 2010). However, anti-inflammatory responses (decreased neutrophilic infiltration) have also been reported in animals instilled *it* with quartz particles following *it* pre-treatment with hydroxylated C60 (Roursgaard et al. 2008), demonstrating that surface modification of this NM can drastically alter its effects *in vivo*. Sayes and colleagues (2007) evaluated the

pulmonary toxicity and local inflammatory responses of C60 aggregates (160 nm diameter) in rats (unspecified strain) at 24 hours, one week, one month, and three months following a single *it* instillation at doses ranging from 0.2 to 3 mg/kg. The only effects reported were transient, with increased percentages of neutrophils in the BAL fluid at 24 hours post-instillation only and increased lipid peroxidation at one day and three months post-exposure. No effects were observed on lactate dehydrogenase, alkaline phosphatase, or total glutathione in the BAL fluid, nor were there any adverse effects noted in lung histopathology.

Effects of NMs on the immune system are of particular concern due to high likelihood of NM uptake by phagocytes such as neutrophils, monocytes, macrophages, and dendritic cells (Patri et al. 2007; Smith et al. 2013b). To date there are few published evaluations of systemic immunotoxic effects following *in vivo* exposure to C60. Yamashita *et al.* (2009) demonstrated that colloidal C60 aggregates (mean diameter: 165 nm) produced a suppression of the delayed-type hypersensitivity (DTH) response to methyl bovine serum albumin in female C57BL/6 mice when administered twice in a dose of 1.1 μg (once before sensitization and once before challenge). Others have reported that *ip* treatment with water-soluble C60 aggregates (ranging from 50 to 250 nm in size) resulted in increased splenocyte production of nitric oxide, decreased splenocyte proliferation, and increased tumor proliferation following inoculation with B16F10 melanoma cells (Zogovic et al. 2009). The production of anti-C60 antibodies of the IgG class in BALB/c mice has also been reported following three immunizations (*ip*) with C60 conjugated to bovine thyroglobulin when administered in Freund's complete and incomplete adjuvants (Chen et al. 1998b).

Due to enormous current and anticipated future development and generation, nanoscale materials were nominated by the Rice University Center for Biological and Environmental Nanotechnology to the National Toxicology Program (NTP) for toxicological testing in 2003 (NTP 2003). As there was insufficient data available regarding the inhalation toxicity of C60 nanoparticles and the potential for differential effects based on particle size, the Division of the NTP of the National Institute of Environmental Health Sciences (NIEHS) selected C60 for evaluation of toxicology and tissue burden following a 13-week nose-only inhalation exposure regimen. Two different C60 aggregate sizes (50 nm and 1 μm diameter) were chosen for testing with exposure concentrations selected to allow for comparisons of toxicity between nanoscale and microscale materials using both mass-based and surface-area-based exposure metrics. The effects of C60 on the lung and the immune system are reported herein. Additional results from these studies describing test material characterization, exposure generation system, atmosphere characterization and C60 lung deposition and clearance are presented elsewhere (Sayers, et al. 2016).

Materials and Methods

Test Article and Exposure Generation System

Details regarding the characterization of the C60 test article and the exposure generation system used in these studies have been previously published in a separate manuscript (Sayers et al. 2016).

Animals

The in-life phase of these studies was conducted at Battelle Toxicology Northwest (Richland, WA, USA) in a facility accredited by the Association for the Assessment and Accreditation of Laboratory Animal Care International (AAALAC). B6C3F1/N mice were obtained from Taconic Farms (Germantown, NY) at approximately 4–5 weeks of age. Wistar Han rats were obtained from Charles River Laboratory (Raleigh, NC) at 4 weeks of age. Animals were maintained on a NTP-2000 diet from (Zeigler Bros., Inc.; Gardners, PA) *ad libitum* except during exposures. See Sayers et al. (2016) for additional information.

Animal use was in accordance with the United States Public Health Service policy on humane care and use of laboratory animals and the Guide for the Care and Use of Laboratory Animals.

Experimental Design

Female animals (n = 16/species/exposure group) were randomly divided into two cohorts (n = 8/cohort/exposure group) for immunotoxicology assessments. The NTP has historically only used female rodents for immunotoxicology studies, as they tend to be more immunologically responsive than their male counterparts, which allows for the detection of subtle immunological effects. A separate group of animals (n = 10/sex/species) was utilized for histopathological analysis. Prior to study onset, animals were placed in the nose-only restraints for up to two hours/day for at least three days to acclimate them to the exposure system. Animals were exposed to C60 fullerene by nose-only inhalation at target concentrations of 0, 0.5 or 2.0 mg/m^3 (50 nm test article-nano-C60) or 0, 2, 15 or 30 mg/m^3 (1.0 μm test article-micro-C60) for 3 hours/day, 5 days/week for 13 weeks. Animals were exposed for 3 hours/day to avoid heat stress. One day after the last exposure to the test article, animals were euthanized via 70% CO_2 inhalation.

Cohort 1—Animals in Cohort 1 were immunized *iv* with sheep red blood cells (sRBC; 3.75×10^8 cells/mL @ 0.2 mL/mouse or 4×10^8 cells/mL @ 0.5 mL/rat) four days prior to sacrifice for evaluation of the T-dependent antibody response (TDAR).

Cohort 2—Animals in Cohort 2 were not immunized and were used to assess all other endpoints, including systemic (spleen cell phenotyping, anti-CD3 mediated T cell proliferation, the mixed leukocyte response [MLR; mice only], and natural killer [NK] cell activity), and local lung-specific effects (BAL cell differentials [rats only] and BAL fluid cytokine analysis). During necropsy, spleens were aseptically removed, placed in individual tubes containing Earle's Balanced Salt Solution (EBBS) with 4-(2-hydroxyethyl)-1-piperazineethanesulfonic acid (HEPES) and gentamicin, and weighed.

Lungs were lavaged twice with 10 mL (rats) or 1 mL (mice) aliquots of Hanks' Balanced Salt Solution (HBSS) with 50 μg/mL gentamicin and the combined lavage fluid was centrifuged (10 min at 360 × g, 4°C). The supernatant portion (i.e. BAL fluid) was frozen at −70°C, and the cell pellet was washed once with 10 mL of HBSS supplemented with gentamicin and resuspended in 1 mL of HBSS with gentamicin. All buffers used for cell

recovery, centrifugation and resuspension were Ca^{2+} and Mg^{2+} free. See supplementary material for additional information.

Histopathology Study Animals—Histopathology study animals underwent a complete necropsy and all major tissues were fixed in 10% neural buffered formalin (NBF), processed and trimmed, embedded in paraffin, sectioned and stained with hematoxylin and eosin (H&E) for microscopic evaluation. The lungs and trachea were infused with 10% NBF up to a normal inspiratory volume prior to fixation and processing. Tissues were examined microscopically (to a no-effect level) from control animals and animals from the highest exposure group. Gross lesions were examined from all exposure groups.

Immunological Studies

Cell Preparation—Spleen cells from animals in the Cohort 1 test groups were resuspended in EBSS with HEPES. Spleen cells and BAL cells from animals in the Cohort 2 test groups were resuspended in Roswell Park Memorial Institute (RPMI) 1640 media supplemented with 10% fetal bovine serum and 5×10^{-5} molar 2-mercaptoethanol ("complete RPMI"). The numbers of nucleated spleen cells and BAL cells for each sample were determined by counting using a Coulter Z2 in the presence of Zap-OGLOBIN II Lytic Reagent (Beckman Coulter, Miami, FL, USA).

T-Dependent Antigen Response to sRBC—The hemolytic plaque assay of Jerne et al. (1963) as modified by White et al. (2010) was used to assess the primary IgM antibody-forming cell (AFC) response to sRBC.

In addition, serum anti-sRBC IgM antibody levels were determined in mice using an enzyme-linked immunosorbent assay (ELISA) as previously described (Temple et al. 1993) with modification (Auttachoat et al. 2009). See supplementary material for additional information.

Spleen Cell Phenotyping—Spleen cells were analyzed by flow cytometry (using a Becton Dickinson FACScan) in order to determine the absolute numbers and percentages of the various cell populations as previously described (Auttachoat et al. 2009). All antibodies were obtained from BD Pharmingen (San Diego, CA). For mice, the antibodies used for the analysis have been previously described (Smith et al. 2013a). For rats, the antibodies used were: OX33 conjugated to fluorescein isothiocyanate (FITC) to enumerate B cells, OX19 conjugated to phycoerythrin (PE) to enumerate T cells ($CD5^+$), OX38 conjugated to FITC to enumerate T-helper cells (T_H; $CD4^+$), and OX8 conjugated to FITC to enumerate cytotoxic T cells (T_{CTL}; $CD8^+$). For both T_H and T_{CTL} cells, a dual label with OX19 was used. For NK cells, a dual label of OX8 conjugated to PE and NKR-P1A antibody conjugated to FITC was used, with NK cells identified by the expression of both markers. Splenic macrophages were labeled with His36 antibody (directed against the rat ED2-like antigen CD163) conjugated to PE.

BAL Cell Phenotyping—Rat BAL cells were stained with His36 antibody conjugated to PE and with anti-CD11b antibody conjugated to FITC. Following staining, cells were analyzed by flow cytometry using a quadrant analysis to determine the absolute numbers

and percentages of double negative ($CD163^{-}CD11b^{-}$), single positive ($CD163^{+}CD11b^{-}$ and $CD163^{-}CD11b^{+}$), and double positive ($CD163^{+}CD11b^{+}$) populations.

Anti-CD3 Proliferation and the Mixed Leukocyte Response—For mice, the T cell proliferative response to anti-CD3 antibody was evaluated as previously described (Smith et al. 2010), using BD Biocoat T cell activation plates (BD Biosciences). For rats, the T cell proliferative response to anti-CD3 antibody was evaluated using the following method: one day before the assay, flat-bottom 96 well plates were coated with anti-rat CD3 antibody (1 μg/ml; 100 μl/well) and incubated overnight at 2–8°C. On the day of the assay, plates were washed with 200 μl of sterile phosphate-buffered saline (PBS) prior to addition of spleen cells. All samples (for both species) were evaluated in quadruplicate cultures in both anti-CD3 treated and non-treated wells. Following culture for two days, all wells were pulsed with 20 μCi ^{3}H-thymidine (1 μCi/well) and cells were harvested 18–24 hours later. The incorporation of ^{3}H-thymidine into proliferating cells was determined, and the data were expressed as counts per minute (CPM)/2×10^{5} cells (mice) or CPM/5×10^{5} cells (rats).

The one-way MLR in mice was conducted in mice only as described previously (Guo et al. 2000). The incorporation of ^{3}H-thymidine into proliferating cells was determined, and the data were expressed as CPM/10^{5} cells.

Bronchoalveolar Lavage Fluid Cytokine Levels—BAL fluid cytokine levels were determined using FlowCytomix™ cytokine bead arrays (eBioscience, San Diego, CA, USA) from a single 25 μl aliquot of each sample according to kit instructions. For rats, the cytokines evaluated were: interleukin (IL)-1α, IL-4, monocyte chemotactic protein (MCP)-1, tumor necrosis factor (TNF)-α, granulocyte-macrophage colony stimulating factor (GM-CSF), and interferon (IFN)-γ. For mice, the cytokines evaluated were: IL-1α, IL-2, IL-4, IL-5, IL-6, IL-10, IL-13, IL-17, MCP-1, IFN-γ, TNF-α, GM-CSF, macrophage inflammatory protein (MIP)-1α, and Regulated upon Activation Normal T cell Expressed and Secreted (RANTES). All cytokine concentrations were quantified using FlowCytomix™ Pro 2.3 software (eBioscience) by interpolation against standard curves generated for each cytokine during analysis. Samples with concentrations below the limit of detection for a cytokine were assigned a value of 0 for that cytokine. See supplementary material for additional information.

Statistical Analysis

Values represent the mean ± standard error (SE) for 8 animals per group (10 for the histopathology studies). Statistical analysis of immunology results (using a mass-based exposure metric) was conducted using Data Entry, Modification, and Statistics Programs Version 6.0 (a proprietary Apple program). Bartlett's Test for homogeneity was used to determine the type of analysis to be conducted. Homogeneous data were analyzed using a one-way analysis of variance (ANOVA), and non-homogeneous data were analyzed using a non-parametric ANOVA. When significant differences occurred, post hoc analysis to determine differences between the control and experimental groups was conducted. For homogeneous data, Dunnett's Test was used for post hoc analysis, while the Wilcoxon Rank Test was used for non-homogeneous data. Jonckheere's Test was used to test for dose-

related trends. The Tukey-Kramer multiple comparison test was used to compare differences among the exposure groups when evaluating BAL cytokine levels. All evaluations using a surface area-based exposure metric were completed using JMP™ 5.0 (SAS Institute, Cary, NC, USA) using the same statistical tests as above and all comparisons were made against a combined control group. The combined control group was used for surface area-based evaluations in order to compare both particle sizes (50 nm and 1 μm). No differences between the controls were observed when statistical differences occurred between exposure groups. The JMP™ software did not offer the Jonckheere's trend analysis and therefore dose-related trends for the surface area-based data were not evaluated. Analysis of histopathological findings was conducted using the Cochran-Armitage Test for dose-related trends and the Fisher's Exact Test for pairwise comparisons with the control group. In all evaluations, $p < 0.05$ indicated statistically significant differences.

Results

Histopathology

The histopathology findings from the lungs and bronchial lymph nodes of male and female Wistar Han rats and B6C3F1/N mice are summarized in Tables 1 and 2, respectively. Histiocytic infiltration consisted of random, multifocal, variably sized clusters of alveolar macrophages within the pulmonary parenchyma, and was graded according to the following criteria: minimal, 0–2 clusters; mild, 3–6 clusters; moderate, 7–10 clusters; marked, >10 clusters. Chronic inflammation was characterized by scattered areas with slightly thickened alveolar septa, few inflammatory cells (lymphocytes, plasma cells, infrequent neutrophils, and alveolar macrophages, often containing pigment), and occasional hypertrophied type II pneumocytes. Severity grading for chronic inflammation was based on the distribution and size of the lesions within the lung, the number of inflammatory cells and hypertrophied type II pneumocytes, and the thickness of the alveolar septa. Pigmentation in the lungs was characterized as brown material free in the alveoli and within alveolar macrophages, and in the lymph nodes as brown pigment within macrophages. It was graded according to the intensity of the pigmentation and the number of pigmented cells present.

In rats exposed to micro-C60 (1 μm), concentration-dependent effects in the incidence and severity of chronic inflammation, histiocytic infiltration and pigmentation in the lung were observed in both sexes; these lesions were observed in all animals following micro-C60 (1 μm) inhalation exposure at 30 mg/m^3. In rats exposed to nano-C60 (50 nm), concentration-dependent effects in histiocytic infiltration and pigmentation in the lung and bronchial lymph node were observed in both sexes. No chronic inflammation was observed in rats following nano-C60 (50 nm) inhalation exposure.

Pigmentation and histiocytic infiltration in the lung were observed in all male and female mice following micro-C60 (1 μm) inhalation exposure concentrations ≥ 15 mg/m^3. Chronic inflammation in the lung was observed in all male mice following micro-C60 (1 μm) inhalation at exposure concentrations ≥ 15 mg/m^3, and in all female mice following micro-C60 (1 μm) inhalation exposure at 30 mg/m^3. Absolute lung weights were significantly increased in females in the 30 mg/m^3 exposure group. Relative lung weights were increased in both sexes in the 30 mg/m^3 exposure groups (data not shown). Pigmentation in the

bronchial lymph nodes was observed in all mice (both sexes) in the 30 mg/m^3 exposure group. In mice exposed to nano-C60 (50 nm), concentration-dependent effects in histiocytic infiltration and pigmentation in the lung and bronchial lymph node were observed in both sexes.

No significant exposure-related neoplastic or non-neoplastic findings were noted in the spleen or the thymus in these studies (data not shown).

Spleen Cell Immunophenotyping

The results of the spleen cell phenotypic analysis conducted in mice exposed to C60 are presented in Table 3 as both mass-based and surface area-based findings; the dose metric can affect interpretation of the results, and therefore the effects were evaluated under both metrics. In terms of absolute values, significant decreases in B cells (18% and 24%) and T cells (20% and 18%) were observed at the 0.5 and 2 mg/m^3 exposure levels of nano-C60 as compared to the control group for the nano-C60, which was consistent with the observed decreases in spleen cell numbers in this group of animals. In animals exposed to micro-C60, no differences were observed in the absolute numbers of the various phenotypes evaluated, with the exception of a significant decrease (22%) in splenic macrophage numbers at the 30 mg/m^3 exposure concentration.

The percentages of splenic T cells, T_H cells, NK cells, and macrophages were unaffected for both C60 aggregate sizes. The percentages of T_{CTL} cells and B cells were unaffected in the nano-C60-exposed mice. For the micro-C60, the percentage of B cells was significantly decreased 8% and 7% for the 2 and 30 mg/m^3 exposure groups, respectively, but not for the 15 mg/m^3 exposure group. The percentage of T_{CTL} cells in the spleens of mice exposed to micro-C60 at 30 mg/m^3 was also significantly decreased (43%).

When the different exposure levels were evaluated together using a surface area-based exposure metric, the decreases in absolute B cell numbers in animals exposed to 0.5 and 2 mg/m^3 of nano-C60 (surface area-based exposures of 0.033 and 0.112 m^2/m^3, respectively) were significantly decreased as compared to control, while differences in absolute numbers of T cells were not statistically significant. Absolute numbers of macrophages were significantly decreased at all exposure concentrations of micro-C60 (0.011, 0.084, and 0.167 m^2/m^3) but not for nano-C60 (0.033 and 0.112 m^2/m^3). The observed significant differences in the percentages and absolute numbers of T_{CTL} cells and the percentages of B cells persisted when evaluated together on a surface area basis.

There were no significant effects on either the absolute values or percentages of the various spleen cell phenotypes evaluated in female rats. See supplementary material for additional information.

TDAR to SRBC

No effects were observed on the numbers of AFC/10^6 splenocytes or on the numbers of AFC/spleen in the plaque assay in either species at any exposure concentration, when evaluated on either a mass exposure basis or surface area exposure basis (Supplementary

Figure S1). Furthermore, the serum levels of anti-sRBC IgM antibodies in mice were unaffected (data not shown). Serum anti-sRBC IgM levels were not evaluated in rats.

BAL Cell Phenotyping

Table 4 gives the results of the phenotyping study conducted on rat BAL cells; mouse BAL cell phenotyping was not conducted. Cells were dually stained with antibodies against the ED2-like antigen CD163 and against CD11b, and a quadrant analysis was used to determine the absolute numbers and percentages of cells expressing one, two, or neither of these markers. No exposure-related effects were observed on the number of cells recovered in the BAL, when evaluated on either a mass basis or on a surface area basis.

When evaluated using a mass-based metric, few effects were observed on the various BAL cell populations evaluated in animals exposed to nano-C60. Neither single-positive population was affected, while the percentage (but not the absolute number) of double-negative cells (i.e. $CD163^{-}CD11b^{-}$) was significantly increased in both nano-C60 exposure groups (8% and 9%, respectively). In addition, significant decreases were observed in the absolute numbers and percentages of double-positive (i.e. $CD163^{+}CD11b^{+}$) cells for both groups of rats exposed to nano-C60. The absolute values of double-positive BAL cells were decreased 86% and 91%, while the percent values were decreased 85% and 90% at the 0.5 and 2 mg/m^3 nano-C60 exposure concentrations.

For the micro-C60 exposed animals, the absolute numbers of double negative cells and both the absolute and percent values of $CD163^{+}CD11b^{-}$ cells were unaffected. The percentages of double-negative BAL cells were increased (22%, 22%, and 11%) at all exposure concentrations, although the increase in the 30 mg/m^3 concentration group failed to reach statistical significance. For $CD163^{-}CD11b^{+}$ cells, both the percent and absolute values were significantly increased (500% and 563%, respectively) in the 30 mg/m^3 concentration group. Finally, the double-positive population was significantly decreased at all exposure groups, with decreases ranging from 94% to 98% for the percent values and from 95% to 98% for the absolute values.

When statistical analysis was conducted using a surface area metric, each of the significant differences observed using the mass metric was again statistically significant. In addition, the percentages of double negative cells were significantly increased in all exposure groups except the 30 mg/m^3 exposure group for micro-C60.

BAL Fluid Cytokines

In the BAL fluid of C60-exposed rats, only two cytokines were altered: MCP-1 and IL-1 (Figure 1). Significant increases in IL-1 levels were observed following exposure to micro-C60 at 15 and 30 mg/m^3 (i.e. 0.084 and 0.167 m^2/m^3) when evaluated based on both mass and surface area exposure (Figure 1, right panel). Furthermore, MCP-1 levels were increased at the highest exposure concentration of micro-C60 using both exposure metrics (Figure 1, left panel). In contrast to the results observed for the micro-C60, no effects were observed on any of the six cytokines evaluated in the BAL fluid of rats exposed to nano-C60 using either metric.

In mice, there were no significant effects on 13 of the 14 cytokines evaluated, including IL-1 and MCP-1, in contrast to the effects observed in C60-exposed rats (data not shown and Supplementary Table S3). The only cytokine affected by C60 exposure in mice was MIP-1α (Figure 2). For this cytokine, when evaluated on a mass basis, statistically significant, concentration-dependent increases of 3,024% and 31,878% were observed in mice exposed to micro-C60 at 15 and 30 mg/m^3, while no increases were observed in animals exposed to nano-C60 (Figure 2). Using a surface area-based metric, MIP-1α levels were increased as compared to the combined control group (517% and 6,212%, respectively) at 15 and 30 mg/m^3 (i.e. 0.084 and 0.167 m^2/m^3) for micro-C60. In addition, levels of this cytokine were significantly increased (217%) over the combined control group for animals exposed to nano-C60 at 2 mg/m^3. Furthermore, MIP-1α levels in the BAL fluid of animals exposed to 0.084 m^2/m^3 (15 mg/m^3 micro-C60) were significantly greater than levels of this cytokine in animals belonging to the 0.112 m^2/m^3 (2 mg/m^3 nano-C60) exposure group.

Discussion

The physicochemical properties of nanomaterials have raised concern for the potential to cause adverse effects following exposure in humans. The size (particle diameter) and surface area of inhaled, insoluble particles have been previously demonstrated to cause differential pathological effects between nanoscale and microscale particles in the lungs of rodents (Oberdorster, 1994). These data suggest that, for studies investigating the toxicity of inhaled nanomaterials, dosimetry (particle surface area or mass) should be an important consideration. The toxicity of C60 fullerene nanoparticles and microparticles following nose-only inhalation was evaluated in this study, with exposure concentrations selected to compare data from both particle sizes using mass-based and particle surface area-based exposure metrics.

The results of the present study demonstrated that inhalation of C60 at concentrations up to 2 mg/m^3 (nano-C60) and 30 mg/m^3 (micro-C60) did not impact systemic immune function in mice or rats, as indicated by a lack of effects on the AFC assay and minimal effects on the numbers of specific cell types in the spleen. The AFC assay, as described in Luster et al (1992), is considered the most sensitive and predictive test of immune function, and, when combined with other immune assays (i.e. plaque forming cell responses and surface marker analysis), is extremely predictive (91% accurate) of systemic immunotoxicity. Decreased spleen cell numbers were observed (on a mass basis) in mice exposed to 2 mg/m^3 nano-C60, however, the total spleen cell number of the control group of mice assigned (randomly) to the 50 nm C60 study was higher than any of the other groups, including the control animals in the 1.0 μm C60 test group, and thus this difference in total spleen cell numbers does not appear to be biologically relevant. Although minimal effects on observational parameters (spleen cell numbers and phenotypes in mice) were noted, these effects were not supported by functional changes and would be scored as equivocal evidence of immunotoxicity based on the NTP Immunotoxicology criteria (NTP, 2009).

In the current study, inflammatory effects (histiocytic infiltration, pigmentation, and chronic inflammation) were noted in lung histopathology. This finding is consistent with previous reports of inflammation induced by C60 particles (Ema et al. 2012; Johnston et al. 2010;

Park et al. 2010). General comparisons of the incidence and average severity results from the lung histopathology evaluations in both rats and mice suggest that the nano-C60 test article initiated a greater inflammatory response compared to micro-C60 test article at the same mass-based exposure for both particle sizes (2 mg/m^3). However, when exposure was evaluated based on surface area, the opposite was observed, in that the micro-C60 test article initiated a greater, or at least similar, inflammatory response at 0.084 m^2/m^3 (15 mg/m^3) in comparison to nano-C60 exposure at a slightly higher surface area-based exposure of 0.112 m^2/m^3 (2 mg/m^3). Although statistical analysis was not conducted using a surface area exposure metric to confirm this observation, the differential effects of nano-C60 and micro-C60 on IL-1 levels (rat) and MIP-1α levels (mouse) support this hypothesis. Furthermore, comparisons of lung burden relative to particle surface area, as described in detail in Sayers et al. (2016), reveal that increasing surface area-based doses correspond with increased particle lung burden. This lends further support to the hypothesis that the inflammatory response following micro-C60 exposure is greater than that for nano-C60 and contrasts with the current paradigm that nanoparticles may be more toxic than microparticles of the same composition.

Significant, concentration-related increases in MCP-1 (rats) and MIP-1α (mice) following C60 inhalation were observed in the present study. These data are consistent with a study demonstrating that C60 inhalation (0.2 mg/m^3) for 4 weeks increased the expression of genes associated with MCP-1 and MIP-1α (Fujita et al. 2009), Interestingly, differential effects were observed in BAL fluid levels of both MIP-1α and MCP-1 between the nano-C60 and micro-C60 exposed animals that could not be accounted for by using surface area as the basis of exposure. MCP-1, also known as chemokine (C-C motif) ligand 2 (CCL2), is a potent chemoattractant for monocytes (Uguccioni et al. 1995). However, MCP-1 has also been shown to have chemoattractant effects on other immune cells, including T cells (Loetscher et al. 1994) and NK cells (Loetscher et al. 1996). MIP-1α, another chemokine, can be secreted by a wide variety of immune cell types, including monocytes and macrophages, T and B cells, NK cells, dendritic cells, neutrophils, and eosinophils (Menten et al. 2002). Increased production of this cytokine is associated with inflammation due to its chemotactic effects on a number of cell types, including monocytes, T cells, neutrophils, eosinophils, basophils, dendritic cells, and NK cells.

The use of CD11b and CD163 in this study for delineating cell types in the BAL fluid did not allow distinct cell types to be determined, as both the double positive and double negative cell populations may contain numerous cell types. Macrophages from different rat tissues typically differ in their expression of various surface antigens, including the MHC class II molecules, CD11b, and CD163 (Dijkstra et al. 1985; Dörger et al. 2001). CD11b is the α-subunit of Mac-1, a β-2 integrin that mediates neutrophil and monocyte adhesion to endothelium, extravasation to sites of inflammation, and phagocytosis processes (Cabañas and Sanchez-Madrid 1999). His36 is an antibody that recognizes the rat ED2-like antigen, which has been identified as the macrophage scavenger receptor CD163 (Polfliet et al. 2006). A phenotyping study evaluating the heterogeneity of tissue macrophage surface marker expression in various tissues of Wistar rats demonstrated that ED2 (CD163) was not expressed by alveolar macrophages (AM) (Dijkstra et al. 1985). A different study using untreated male Crl:CD rats indicated that rat AM expressed low levels of both CD11b and

CD163, while both of these markers were highly expressed in pleural and peritoneal macrophages (Dörger et al. 2001). Similar results in a study of AM from untreated Fisher 344 rats demonstrated low surface expression of CD11b, while CD163 expression was absent (Garn et al. 2006). In light of these reports, it is most likely that the double negative (i.e. $CD163^{-}CD11b^{-}$) population of rat BAL cells in the present study consisted primarily of AM, in addition to a smaller population of other cell types, including T and B lymphocytes, NK cells, eosinophils, and mast cells, which can all be recovered from BAL in low numbers (Dörger et al. 2001). Cells staining positive for both CD163 and CD11b were most likely a combination of resident airway macrophages, which have been identified throughout the respiratory tract (Sibille and Reynolds 1990), and macrophages recruited to the lung. Cells staining positive for CD11b only (i.e. $CD163^{-}CD11b^{+}$) were neutrophils and other myeloid cells.

Significant increases in the percentage and absolute numbers of $CD163^{-}CD11b^{+}$ neutrophils were observed in rats exposed to 30 mg/m^3 micro-C60, which correlated with a significant increase in neutrophils in rats in the same exposure group identified by BAL fluid differential cell counting (Supplementary Table S2). Unfortunately, cellular origin is not determined for macrophages identified by differential cell counting. In a study by Garn et al. (2006), phenotyping of BAL macrophages from Fisher 344 rats that had received an inflammatory insult (NO_2 inhalation) demonstrated an exposure-related increase in $CD11b^{+}$ cells. The authors suggested this was due either to increased expression of that marker by AM or to the infiltration of $CD11b^{+}$ monocytes/macrophages. In light of the increased MCP-1 levels in our study (a cytokine that serves, in part, to increase the number of monocytes and macrophages in the lung), it is more likely that the increase in $CD11b^{+}$ cells is the result of cellular infiltration (e.g. monocytes/macrophages and neutrophils) and not a change in surface marker expression by resident AM. This is further supported by reports that, under inflammatory conditions (Li et al. 1998) and non-inflammatory conditions following instillation of MCP-1 (Maus et al. 2001), $CD11b^{+}$ monocytes that are distinct from resident AM can migrate into the alveoli.

MIP-1α is believed to contribute significantly to sustaining cell recruitment during inflammatory responses, and increases in this cytokine are associated with increased monocyte adhesion to tissue endothelium (Menten et al. 2002). MCP-1 also increases both monocyte adhesion via the CD11b/CD18 integrin (Weber et al. 1999) and expression of CD11b in human peripheral blood monocytes (Jiang et al. 1992). Conversely, engagement of CD163 and/or CD11b is known to initiate or up-regulate the secretion of inflammatory cytokines, including IL-1, IL-6, MIP-1α, and TNF-α (Fan and Edgington 1993; Polfliet et al. 2006; Rezzonico et al. 2001), suggesting a positive feedback loop of sorts between inflammatory cytokine production and expression of CD11b and CD163. Interestingly, $CD163^{+}$ macrophages play a dual role in inflammatory responses (Akila et al. 2012). Increasing numbers of macrophages expressing CD163 are often found in the late and resolution phases of an inflammatory reaction and, in response to increased levels of nitric oxide and IL-6, begin secreting anti-inflammatory cytokines like IL-10 (Akila et al. 2012; Fabriek et al. 2005).

C60 inhalation in the present study resulted in significant, dramatic decreases in the absolute number and percentage of $CD163^{+}CD11b^{+}$ macrophages in all groups of C60-exposed rats without regard to exposure concentration. The drastic decreases observed in $CD163^{+}CD11b^{+}$ macrophages in our study were unexpected. The logical expectation would be that the number of these cells would increase in response to increased levels of monocyte/macrophage chemokines. However, the results show quite the opposite. The reasons for these decreases, which were equally large at all C60 exposure concentrations, are unknown. It is possible that, because of the high levels of inflammatory cytokines, β-2 integrin-mediated adherence of these cells to the lung endothelium may have increased significantly, such that the cells were not readily detached and collected during lavage. Alternatively, perhaps monocytes infiltrating into the lung matured into AM, which do not express CD163. The decreased numbers and percentages of $CD163^{+}$ macrophages in the BAL may also be an "adaptive" response to the extended repetitive nature of the particulate exposure. Specifically, because $CD163^{+}$ macrophages can contribute to anti-inflammatory responses, particularly in the presence of IL-6 and nitric oxide (Akila et al. 2012), repeated inhalation of particulate matter over the 13-week exposure period may have promoted a decrease in $CD163^{+}$ macrophages in order to decrease anti-inflammatory cytokine production.

These studies have demonstrated that the immune effects of C60 fullerene inhalation in rats and mice were limited primarily to the lung, where dramatically increased levels of the monocyte/macrophage chemotactic and inflammatory cytokines MCP-1 and MIP-1α were detected in BAL fluid. Increases in MCP-1 and MIP-1α have been linked to the formation of pulmonary fibrosis in rodents and humans (Hasegawa 1999; Menten et al. 2002; Smith et al. 1995). In fact, the absence of MCP-1 in $CCL2^{-/-}$ mice conferred protection against bleomycin-induced pulmonary fibrosis (Baran et al. 2007). In humans, pneumoconiosis, or particle-induced pulmonary fibrosis, has been documented in several cases of occupational exposure to particulates, although there are no documented human cases of pulmonary fibrosis directly linked to NM exposure (Byrne and Baugh 2008). However, NM-mediated pulmonary fibrosis has been observed in Sprague Dawley rats as soon as 21 days and persisting for at least 60 days following a single *it* instillation of multiwalled carbon nanotubes (MWCNT) (Cesta et al. 2010; Muller et al. 2005). Further, it has been suggested that nanoparticles are the fraction of inhaled particulates that contribute most significantly to pulmonary fibrosis in humans (Byrne and Baugh 2008).

Conclusion

C60 fullerene inhalation in both rats and mice for 13 weeks had little effect on systemic immune function. Locally, lung inflammatory responses were observed, primarily at the higher exposure concentrations. Increased pulmonary inflammation and cytokine levels in the BAL further the concern over increasing exposure to NMs. Inflammatory effects of nano-C60 exposure were, in general, more severe than micro-C60 exposure when comparing both particle sizes at the same mass-based exposure. However, the opposite pattern was evident with a surface area-based exposure evaluation. These data highlight the importance of dosimetry when evaluating toxicity between nano- and microparticles.

Supplementary Material

Refer to Web version on PubMed Central for supplementary material.

Acknowledgments

Special thanks to Ronnetta Brown, Deborah Musgrove, Dr. Wimolnut Auttachoat, and Dr. Tai Guo for their contributions to these studies. The authors also thank Drs. Susan Elmore and William Gwinn for their thoughtful and critical review of this manuscript.

Abbreviations

AAALAC	Association for the Assessment and Accreditation of Laboratory Animal Care International
AFC	antibody-forming cell
AM	alveolar macrophage
ANOVA	analysis of variance
BAL	bronchoalveolar lavage
CCL2	chemokine (C-C motif) ligand-2
CPM	counts per minute
EBSS	Earle’s Balanced Salt Solution
ELISA	enzyme-linked immunosorbent assay
EU	European Union
F	female
FDA	U.S. Food and Drug Administration
FITC	fluorescein isothiocyanate
GM-CSF	granulocyte-macrophage colony stimulating factor
HEPES	4-(2-hydroxyethyl)-1-piperazineethanesulfonic acid
IFN-γ	interferon
IgG	immunoglobulin G
IgM	immunoglobulin M
IL	interleukin
ip	intraperitoneal
it	intratracheal
M	male

MCP-1	monocyte chemoattractant protein-1
MIP-1α	macrophage inflammatory protein-1 alpha
MLR	mixed leukocyte response
NIEHS	National Institute of Environmental Health Sciences
NK	natural killer
NM	nanomaterial
NTP	National Toxicology Program
OD	optical density
PBS	phosphate-buffered saline
PE	phycoerythrin
RANTES	Regulated upon Activation Normal T cell Expressed and Secreted
RPMI	Roswell Park Memorial Institute
SE	standard error
sRBC	sheep red blood cells
T_{CTL}	cytotoxic T cell
TDAR	T-dependent antibody response
T_H	helper T cell
TNF-α	tumor necrosis factor
VCU	Virginia Commonwealth University

References

Akila P, Prashant V, Suma MN, Prashant SN, Chaitra TR. CD163 and its expanding functional repertoire. Clin Chim Acta. 2012; 413:669–674. [PubMed: 22309681]

Auttachoat W, Germolec DR, Collins BJ, Luebke RW, White KL Jr, Guo TL. Immunotoxicological profile of chloroform in female B6C3F1 mice when administered in drinking water. Drug Chem Toxicol. 2009; 32:77–87. [PubMed: 19514942]

Baker GL, Gupta A, Clark ML, Valenzuela BR, Staska LM, Harbo SJ, Pierce JT, Dill JA. Inhalation toxicity and lung toxicokinetics of C60 fullerene nanoparticles and microparticles. Toxicol Sci. 2008; 101:122–131. [PubMed: 17878152]

Balbus JM, Maynard AD, Colvin VL, Castranova V, Daston GP, Denison RA, Dreher KL, Goering PL, Goldberg AM, Kulinowski KM, Monteiro-Riviere NA, Oberdorster G, Omenn GS, Pinkerton KE, Ramos KS, Rest KM, Sass JB, Silbergeld EK, Wong BA. Meeting report: hazard assessment for nanoparticles--report from an interdisciplinary workshop. Environ Health Perspect. 2007; 115:1654–1659. [PubMed: 18007999]

Baran CP, Opalek JM, McMaken S, Newland CA, O'Brien JM, Hunter MG, Bringardner BD, Monick MM, Brigstock DR, Stromberg PC, Hunninghake GW, Marsh CB. Important roles for macrophage

colony-stimulating factor, CC chemokine ligand 2, and mononuclear phagocytes in the pathogenesis of pulmonary fibrosis. Am J Respir Crit Care Med. 2007; 176:78–89. [PubMed: 17431224]

Bide RW, Armour SJ, Yee E. Allometric respiration/body mass data for animals to be used for estimates of inhalation toxicity to young adult humans. J Appl Toxicol. 2000; 20:273–290. [PubMed: 10942903]

Bleeker EAJ, de Jong WH, Geertsma RE, Groenewold M, Heugens EHW, Koers-Jacquemijns M, van de Meent D, Popma JR, Rietveld AG, Wijnhoven SWP, Cassee FR, Oomen AG. Considerations on the EU definition of a nanomaterial: science to suppot policy making. Regul Toxicol Pharm. 2013; 65:119–125.

Byrne JD, Baugh JA. The significance of nanoparticles in particle-induced pulmonary fibrosis. Mcgill J Med. 2008; 11:43–50. [PubMed: 18523535]

Cabañas C, Sanchez-Madrid F. CD11b (leukocyte integrin CR3 alpha subunit). J Biol Reg Homeos Ag. 1999; 13:130–133.

Cesta MF, Ryman-Rasmussen JP, Wallace DG, Masinde T, Hurlburt G, Taylor AJ, Bonner JC. Bacterial lipopolysaccharide enhances PDGF signaling and pulmonary fibrosis in rats exposed to carbon nanotubes. Am J Respir Cell Mol Biol. 2010; 43:142–151. [PubMed: 19738159]

Chen HH, Yu C, Ueng TH, Chen S, Chen BJ, Huang KJ, Chiang LY. Acute and subacute toxicity study of water-soluble polyalkylsulfonated C60 in rats. Toxicol Pathol. 1998a; 26:143–151. [PubMed: 9502397]

Chen BX, Wilson SR, Das M, Coughlin DJ, Erlanger BF. Antigenicity of fullerenes: antibodies specific for fullerenes and their characteristics. Proc Natl Acad Sci U S A. 1998b; 95:10809–10813. [PubMed: 9724786]

Dijkstra CD, Döpp EA, Joling P, Krall G. The heterogeneity of mononuclear phagocytes in lymphoid organs: distinct macrophage subpopulations in the rat recognized by monoclonal antibodies ED1, ED2 and ED3. Immunology. 1985; 54:589–599. [PubMed: 3882559]

Dörger M, Münzing S, Allmeling A, Messmer K, Krombach F. Phenotypic and functional differences between rat alveolar, pleural, and peritoneal macrophages. Exp Lung Res. 2001; 27:65–76. [PubMed: 11202064]

Ema M, Tanaka J, Kobayashi N, Naya M, Endoh S, Maru J, Hosoi M, Nagai M, Nakajima M, Hayashi M, Nakanishi J. Genotoxicity evaluation of fullerene C60 nanoparticles in a comet assay using lung cells in intratracheally instilled rats. Regul Toxicol Pharm. 2012; 62:419–424.

EU. Commission recommendation of 18 October 2011 on the definition of nanomaterial (2011/696/EU). Official Journal of the European Union. 2011; L275:38–40.

Fabriek BO, Dijkstra CD, van den Berg TK. The macrophage scavenger receptor CD163. Immunobiology. 2005; 210:153–160. [PubMed: 16164022]

Fan ST, Edgington TS. Integrin regulation of leukocyte inflammatory functions. CD11b/CD18 enhancement of the tumor necrosis factor-alpha responses of monocytes. J Immunol. 1993; 150:2972–2980. [PubMed: 8095957]

FDA. [Accessed online on May 27, 2014] Considering whether an FDA-regulated product involves the application of nanotechnology. Guidance for Industry (Draft). 2011. at www.fda.gov/RegulatoryInformation/Guidances/ucm257698.htm

Fujita K, Morimoto Y, Ogami A, Toshihiko M, Tanaka I, Shimada M, Wang W, Endoch S, Uchida K, Nakazato T, Yamamoto K, Fukui H, Horie M, Yoshida Y, Iwahashi H, Nakanishi J. Gene expression profiles in rat lung after inhalation exposure to C60 fullerene particles. Toxicology. 2009; 258:47–55. [PubMed: 19167457]

Garn H, Siese A, Stumpf S, Wensing A, Renz H, Gemsa D. Phenotypical and functional characterization of alveolar macrophage subpopulations in teh lungs of NO2-exposed rats. Respir Res. 2006; 7:4. [PubMed: 16398938]

Guo TL, McCay JA, Brown RD, Musgrove DL, Butterworth L, Munson AE, Germolec DR, White KL Jr. Glycidol modulation of the immune responses in female B6C3F1 mice. Drug and Chemical Toxicology. 2000; 23:433–457. [PubMed: 10959546]

Hasegawa M. Augmented production of chemokines (monocyte chemotactic protein-1 (MCP-1), macrophage inflammatory protein-1alpha (MIP-1alpha) and MIP-1beta) in patients with systemic

sclerosis: MCP-1 and MIP-1alpha may be involved in the development of pulmonary fibrosis. Clin Exp Immunol. 1999; 117:159–165. [PubMed: 10403930]

Jerne, NK.; Nordin, AA.; Henry, C. The agar plaque technique for recognizing antibody-producing cells. In: Amos, B.; Koprowski, H., editors. Cell-Bound Antibodies. Wistar Institute Press; Philadelphia: 1963. p. 109-125.

Jiang Y, Beller DI, Frendl G, Graves DT. Monocyte chemoattractant protein-1 regulates adhesion molecule expression and cytokine production in human monocytes. J Immunol. 1992; 148:2423–2428. [PubMed: 1348518]

Johnston HJ, Hutchison GR, Christensen FM, Aschberger K, Stone V. The biological mechanisms and physicochemical characteristics responsible for driving fullerene toxicity. Toxicol Sci. 2010; 114:162–182. [PubMed: 19901017]

Kawabata TT, Babcock LS, Gauggel DL, Asquith TN, Fletcher ER, Horn PA, Ratajczak HV, Graziano FM. Optimization and validation of an ELISA to measure specific guinea pig IgG1 antibody as an alternative to the in vivo passive cutaneous anaphylaxis assay. Fundam Appl Toxicol. 1995; 24:238–246. [PubMed: 7737435]

Kroto HW, Heath JR, O'Brien SC, Curl RF, Smalley RE. C60: buckminsterfullerene. Nature. 1985; 318:162–163.

Li XC, Miyasaka M, Issekutz T. Blood monocyte migration to acute lung inflammation involves both CD11/CD18 and very late activiation antigen-4-dependent and independent pathways. J Immunol. 1998; 161:6258–6264. [PubMed: 9834114]

Loetscher P, Seitz M, Clark-Lewis I, Baggiolini M, Moser B. Monocyte chemotactic proteins MCP-1, MCP-2, and MCP-3 are major attractants for human CD4+ and CD8+ T lymphocytes. Faseb J. 1994; 8:1055–1060. [PubMed: 7926371]

Loetscher P, Seitz M, Clark-Lewis I, Baggiolini M, Moser B. Activation of NK cells by CC chemokines. Chemotaxis, Ca2+ mobilization, and enzyme release. J Immunol. 1996; 156:322–327. [PubMed: 8598480]

Luster MI, Portier C, Pait DG, White KL Jr, Gennings C, Munson AE, Rosenthal GJ. Risk assessment in immunotoxicology I: Sensitivity and predictability of immune tests. Fundam Appl Toxicol. 1992; 18:200–210. [PubMed: 1534777]

Maus U, Herold S, Muth H, Maus R, Ermert L, Ermert M, Weissman N, Rousseau S, Seeger W, Grimminger F, Lohmeyer J. Monocytes recruited into the alveolar air space of mice show a monocytic phenotype but upregulate CD14. Am J Physiol Lung Cell Mol Physiol. 2001; 280:L58–68. [PubMed: 11133495]

Menten P, Wuyts A, Van Damme J. Macrophage inflammatory protein-1. Cytokine Growth F R. 2002; 13:455–481.

Muller J, Huaux F, Moreau N, Mission P, Heilier JF, Delos M, Arras M, Fonseca A, Nagy JB, Lison D. Respiratory toxicity of multi-wall carbon nanotubes. Toxicol Appl Pharmacol. 2005; 207:221–231. [PubMed: 16129115]

National Toxicology Program (NTP). [Last accessed September 5, 2014] Nanoscale materials. Nominations to the Testing Program, Nominations in Review 2003. 2003. Internet address: http://ntp.niehs.nih.gov/ntp/htdocs/Chem_Background/ExSumPdf/Nanoscale_508.pdf

National Toxicology Program (NTP). [Last accessed July 26, 2016] Evaluation Criteria for Immune System Toxicity. 2009. Internet address: http://ntp.niehs.nih.gov/testing/types/criteria/

Park EJ, Kim H, Kim Y, Yi J, Choi K, Park K. Carbon fullerenes (C60s) can induce inflammatory responses in the lung of mice. Toxicol Appl Pharmacol. 2010; 244:226–233. [PubMed: 20064541]

Patri, A.; Dobrovolskaia, M.; Stern, S.; McNeil, S. Preclinical Characterization of Engineered Nanoparticles Intended for Cancer Therapeutics. In: Amiji, MM., editor. Nanotechnology for Cancer Therapy. CRC Press; 2007. p. 105-137.

Polfliet MMJ, Fabriek BO, Daniëls WP, Dijkstra CD, van den Berg TK. The rat macrophage scavenger receptor CD163: Expression, regulation, and role in inflammatory mediator production. Immunobiology. 2006; 211:419–425. [PubMed: 16920481]

Rezzonico R, Imbert V, Chicheportiche R, Dayer JM. Ligation of CD11b and CD11c beta(2) integrins by antibodies or soluble CD23 induces macrophage inflammatory protein 1alpha (MIP-1alpha)

and MIP-1beta production in primary human monocytes through a pathway dependent on nuclear factor-kappaB. Blood. 2001; 97:2932–2940. [PubMed: 11342414]

Roursgaard M, Poulsen SS, Kepley CL, Hammer M, Nielsen GD, Larsen ST. Polyhydroxylated C60 fullerene (fullerenol) attenuates neutrophilic lung inflammation in mice. Basic Clin Pharmacol Toxicol. 2008; 103:386–388. [PubMed: 18793270]

Sayers BC, Walker NJ, Roycroft JH, Germolec DR, Baker GL, Clark ML, Hayden BK, DeFord H, Dill JA, Gupta A, Stout MD. Lung deposition and clearance of microparticle and nanoparticle C60 fullerene aggregates in B6C3F1 mice and Wistar Han rats following nose-only inhalation for 13 weeks. Toxicology. 2016; 339:87–96. [PubMed: 26612504]

Sayes CM, Marchione AA, Reed KL, Warheit DB. Comparative pulmonary toxicity assessments of C60 water suspensions in rats: few differences in fullerene toxicity in vivo in contrast to in vitro profiles. Nano Lett. 2007; 7:2399–2406. [PubMed: 17630811]

Shinohara N, Gamo M, Nakanishi J. Fullerene C60: Inhalation hazard assessment and derivation of a period-limited acceptable exposure level. Toxicol Sci. 2011; 123:576–589. [PubMed: 21856993]

Sibille Y, Reynolds HY. Macrophages and polymorphonuclear neutrophils in lung defense and injury. Am Rev Respir Dis. 1990; 141:471–501. [PubMed: 2405761]

Smith DC, Smith MJ, White KL. Systemic Immunosuppression Following a Single Pharyngeal Aspiration of 1,2:5,6-Dibenzanthracene in Female B6C3F1 Mice. J Immunotoxicol. 2010; 7:219–231. [PubMed: 20509767]

Smith MJ, Germolec DR, Frawley RP, White KL. Immunomodulatory effects of black cohosh (Actaea racemosa) extract in female B6C3F1/N mice. Toxicology. 2013a; 308:146–157. [PubMed: 23571075]

Smith, MJ.; McLoughlin, CE.; White, KL.; Germolec, DR. Evaluating the adverse effects of nanomaterials on the immune system with animal models. In: Dobrovolskaia, MA.; McNeil, SE., editors. Handbook of Immunological Properties of Engineered Nanomaterials. World Scientific; New Jersey: 2013b. p. 639-670.

Smith RE, Strieter RM, Zhang K, Phan SH, Standiford TJ, Lukacs NW, Kunkel SL. A role for C-C chemokines in fibrotic lung disease. J Leukoc Biol. 1995; 57:782–787. [PubMed: 7539030]

Temple L, Kawabata TT, Munson AE, White KL Jr. Comparison of ELISA and plaque-forming cell assays for measuring the humoral immune response to SRBC in rats and mice treated with benzo[a]pyrene or cyclophosphamide. Fundam Appl Toxicol. 1993; 21:412–419. [PubMed: 8253294]

Terrones H, Mackay AL. The geometry of hypothetical curved graphite structures. Carbon. 1992; 30:1251–1260.

Uguccioni M, D'Apuzzo M, Loetscher M, Dewald B, Baggiolini M. Actions of the chemotactic cytokines MCP-1, MCP-2, MCP-3, RANTES, MIP-1 alpha and MIP-1 beta on human monocytes. Eur J Immunol. 1995; 25:64–68. [PubMed: 7531149]

Weber KS, Klickstein LB, Weber C. Specific activation of leukocyte beta2 integrins lymphocyte function-associated antigen-1 and Mac-1 by chemokines mediated by distinct pathways via the alpha subunit cytoplasmic domains. Mol Biol Cell. 1999; 10:861–873. [PubMed: 10198043]

White KL, Musgrove DL, Brown RD. The Sheep Erythrocyte T-Dependent Antibody Response (TDAR). Methods Mol Biol. 2010; 598:173–184. [PubMed: 19967513]

Yamashita K, Sakai M, Takemoto N, Tsukimoto M, Uchida K, Yajima H, Oshio S, Takeda K, Kojima S. Attenuation of delayed-type hypersensitivity by fullerene treatment. Toxicology. 2009; 261:19–24. [PubMed: 19376187]

Zogovic NS, Nikolic NS, Vranjes-Djuric SD, Harhaji LM, Vucicevic LM, Janjetovic KD, Misirkic MS, Todorovic-Markovic BM, Markovic ZM, Milonjic SK, Trajkovic VS. Opposite effects of nanocrystalline fullerene (C(60)) on tumour cell growth in vitro and in vivo and a possible role of immunosupression in the cancer-promoting activity of C(60). Biomaterials. 2009; 30:6940–6946. [PubMed: 19781768]

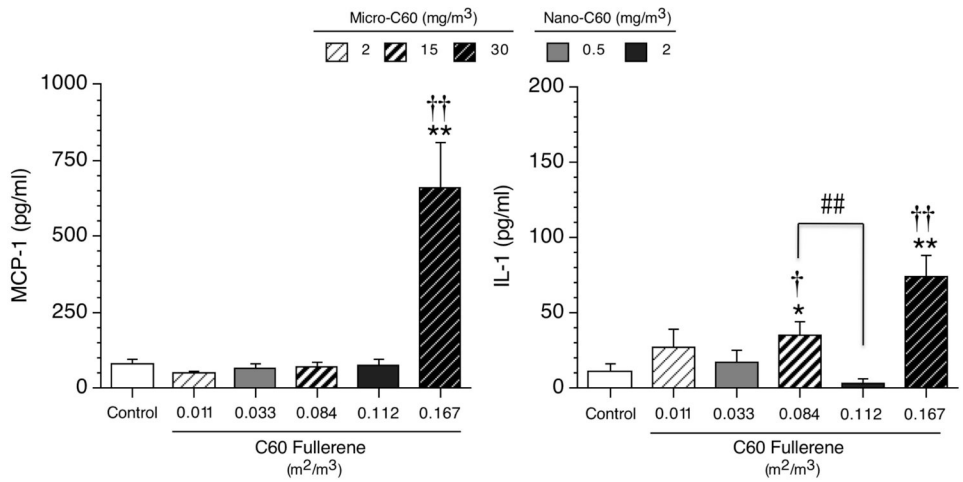

Figure 1. MCP-1 and IL-1 levels in the BAL fluid of female Wistar Han rats following C60 fullerene inhalation for 13 weeks

Combined control group results are shown. Values of control animals assigned to the micro-C60 and nano-C60 studies were not significantly different. Individual study control values (pg/ml) for MCP-1 were: 65 ± 22 (micro-C60 study) and 93 ± 24 (nano-C60 study). Individual study control values (pg/ml) for IL-1 were: 4 ± 4 (micro-C60 study) and 18 ± 9 (nano-C60 study). Values represent the mean ± SE (N = 8 animals per test group; N = 16 for combined control group). Significant differences from individual study control group (not shown): *$p < 0.05$ and **$p < 0.01$. Significant differences from combined control group (shown): $^{\dagger}p < 0.05$ and $^{\dagger\dagger}p < 0.01$. Pairwise significant differences between C60 exposure groups: $^{\#\#}p < 0.01$.

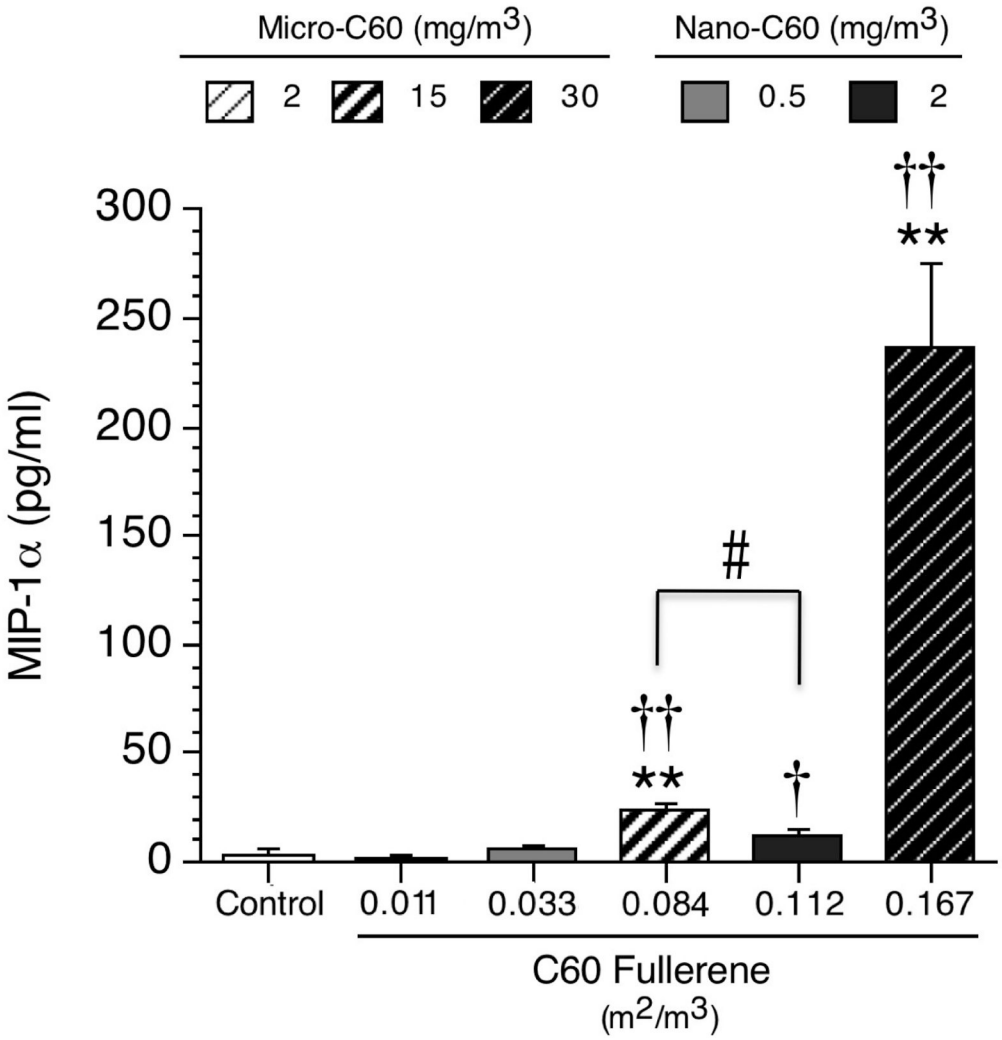

Figure 2. MIP-1α levels in the BAL fluid of female B6C3F1/N mice following C60 fullerene inhalation for 13 weeks

Combined control group results are shown. Values of control animals assigned to the micro-C60 and nano-C60 studies were not significantly different. Individual study control values (pg/ml) were: 0.74 ± 0.7 (micro-C60 study) and 6.8 ± 3.3 (nano-C60 study). Values represent the mean ± SE (N = 8 animals per test group; N = 16 for combined control group). Significant differences from individual study control group (not shown): $^{**}p < 0.01$. Significant differences from combined control group (shown): $^{\dagger}p < 0.05$ and $^{\dagger\dagger}p < 0.01$. Pairwise significant differences between C60 exposure groups: $^{\#}p < 0.05$.

Table 1

Incidence and severity of lung and lymph node non-neoplastic lesions in Wistar Han rats

	Control	C60 Fullerene (m^2/m^3)				
		0.011	0.033	0.084	0.112	0.167
Male Wistar Han rats						
50 nm C60						
Mass-Based Exp. Conc. (mg/m^3)	*0*	-	*0.5*	-	*2*	-
Lung						
Weight (g)	2.15 ± 0.31		2.18 ± 0.50		2.06 ± 0.39	
Histiocytic Infiltration	1/10 (1.0)	-	1/10 (1.0)	-	3/10 (1.3)	-
Osseous Metaplasia	1/10 (1.0)	-	0/10	-	0/10	-
Pigmentation	0/10	-	0/10	-	3/10 (1.0)	-
Lymph Node Pigmentation						
Bronchial	0/10	-	3/9 (1.0)	-	4/10 (1.0)	-
Mediastinal	1/10 (1.0)	-	6/8 (1.0)	-	2/10 (1.0)	
1 μm C60						
Mass-Based Exp. Conc. (mg/m^3)	*0*	*2*	-	*15*	-	*30*
Lung						
Weight (g)	2.20 ± 0.48	1.90 ± 0.33		2.06 ± 0.49		2.30 ± 0.31
Histiocytic Infiltration	1/10 (1.0)	1/10 (1.0)	-	8/9 (1.4)	-	10/10 (3.8)
Chronic Inflammation	1/10 (1.0)	4/10 (1.0)	-	8/9 (1.8)	-	10/10 (2.0)
Pigmentation	0/10	1/10 (1.0)	-	8/9 (2.1)	-	10/10 (3.2)
Lymph Node Pigmentation						
Bronchial	0/7	1/5 (1.0)	-	3/6 (1.0)	-	7/8 (1.9)
Mediastinal	4/8 (1.0)	4/9 (1.0)	-	3/8 (1.7)	-	5/9 (1.6)
Female Wistar Han rats						
50 nm C60						
Mass-Based Exp. Conc. (mg/m^3)	*0*	-	*0.5*	-	*2*	-
Lung						
Weight (g)	1.46 ± 0.28		1.43 ± 0.21		1.55 ± 0.35	

	Control	C60 Fullerene (m^2/m^3)				
		0.011	**0.033**	**0.084**	**0.112**	**0.167**
Histiocytic Infiltration	2/10 (1.0)	-	1/10 (1.0)	-	8/10 (1.0)	-
Osseous Metaplasia	2/10 (1.0)	-	1/10 (1.0)	-	0/10	-
Pigmentation	0/10	-	0/10	-	8/10 (2.0)	-
Lymph Node Pigmentation						
Bronchial	0/10	-	1/10 (1.0)	-	5/10 (1.2)	-
Mediastinal	0/8	-	7/8 (1.0)	-	9/10 (1.3)	
1 μm C60						
Mass-Based Exp. Conc. (mg/m³)	*0*	*2*	-	*15*	-	*30*
Lung						
Weight (g)	1.54 ± 0.36	1.48 ± 0.24		1.56 ± 0.25		1.63 ± 0.33
Histiocytic Infiltration	1/10 (1.0)	1/10 (1.0)	-	8/10 (1.0)	-	10/10 (4.0)
Chronic Inflammation	0/10	0/10	-	1/10 (1.0)	-	10/10 (2.0)
Pigmentation	0/10	0/10	-	8/10 (2.3)	-	10/10 (3.2)
Lymph Node Pigmentation						
Bronchial	1/6 (1.0)	1/5 (1.0)	-	3/7 (1.3)	-	4/5 (1.5)
Mediastinal	3/8 (1.0)	9/10 (1.1)	-	7/8 (1.3)	-	7/9 (1.6)

Mass-Based Exp. Conc. = Mass-Based Exposure Concentration

Values represent incidence/number examined

Values in parentheses represent average severity grade (1-minimal; 2-mild; 3-moderate; 4-marked)

Table 2

Incidence and severity of lung and lymph node non-neoplastic lesions in B6C3F1/N mice

	Control	C60 Fullerene (m^2/m^3)				
		0.011	0.033	0.084	0.112	0.167
Male B6C3F1/N mice						
50 nm C60						
Mass-Based Exp. Conc. (mg/m^3)	*0*	-	*0.5*	-	*2*	-
Lung						
Weight (g)	0.20 ± 0.01		0.20 ± 0.02		0.20 ± 0.02	
Histiocytic Infiltration	1/10 (1.0)	-	2/10 (1.0)	-	7/10 (2.3)	-
Chronic Inflammation	0/10	-	0/10	-	1/10 (1.0)	-
Pigmentation	0/10	-	0/10	-	7/10 (2.9)	-
Lymph Node Pigmentation						
Bronchial	0/9	-	2/7 (1.0)	-	5/7 (1.0)	-
1 μm C60						
Mass-Based Exp. Conc. (mg/m^3)	*0*	*2*	-	*15*	-	*30*
Lung						
Weight (g)	0.19 ± 0.02	0.20 ± 0.03		0.19 ± 0.03		0.21 ± 0.02
Histiocytic Infiltration	0/10	0/10	-	10/10 (2.9)	-	10/10 (3.9)
Chronic Inflammation	0/10	0/10	-	10/10 (1.0)	-	10/10 (1.9)
Pigmentation	0/10	0/10	-	10/10 (3.2)	-	10/10 (3.8)
Lymph Node Pigmentation						
Bronchial	2/6 (1.0)	1/4 (1.0)	-	2/5 (1.0)	-	9/9 (2.9)
Female B6C3F1/N mice						
50 nm C60						
Mass-Based Exp. Conc. (mg/m^3)	*0*	-	*0.5*	-	*2*	-
Lung						
Weight (g)	0.20 ± 0.01		0.22 ± 0.04		0.20 ± 0.03	
Histiocytic Infiltration	2/10 (1.5)	-	1/10 (1.0)	-	5/10 (1.0)	-
Chronic Inflammation	0/10	-	1/10 (1.0)	-	0/10	-

	Control	C60 Fullerene (m^2/m^3)				
		0.011	**0.033**	**0.084**	**0.112**	**0.167**
Pigmentation	0/10	-	0/10	-	5/10 (2.4)	-
Lymph Node Pigmentation						
Bronchial	2/10 (1.0)	-	3/7 (1.0)	-	4/10 (1.0)	-
1 μm C60						
Mass-Based Exp. Conc. (mg/m^3)	*0*	*2*	-	*15*	-	*30*
Lung						
Weight (g)	0.19 ± 0.01	0.19 ± 0.02		0.19 ± 0.01		0.22 ± 0.02 *
Histiocytic Infiltration	0/10	0/10	-	10/10 (2.4)	-	10/10 (4.0)
Chronic Inflammation	0/10	0/10	-	3/10 (1.0)	-	10/10 (2.0)
Pigmentation	0/10	0/10	-	10/10 (2.9)	-	10/10 (4.0)
Lymph Node Pigmentation						
Bronchial	2/5 (1.0)	3/6 (1.0)	-	1/5 (1.0)	-	6/6 (2.7)

Mass-Based Exp. Conc. = Mass-Based Exposure Concentration

Values represent incidence/number examined

Values in parentheses represent average severity grade (1-minimal; 2-mild; 3-moderate; 4-marked)

* $p \leq 0.01$

Table 3

Spleen cell phenotypes in female B6C3F1/N mice following 13-week inhalation of C60

	Control	C60 Fullerene (m^2/m^3)					Trend Analysis
		0.011	0.033	0.084	0.112	0.167	
Absolute Values ($\times 10^6$)							
50 nm C60							
Mass-Based Exp. Conc. (mg/m^3)	*0*	-	*0.5*	-	*2*	-	-
Spleen Cells ($\times 10^6$)	174.0 ± 8.2	-	161.3 ± 7.0	-	144.8 ± 4.5 *	-	$p \leq 0.01$
[a] Ig^+	112.5 ± 4.3	-	92.5 ± 4.0 **†	-	85.4 ± 3.4 **††	-	$p \leq 0.01$
[b] $CD3^+$	28.2 ± 1.7	-	22.5 ± 1.1 *	-	23.1 ± 1.2 *	-	$p \leq 0.05$
[c] $CD4^+CD8^-$	18.4 ± 1.2	-	15.5 ± 0.8	-	15.8 ± 0.9	-	NS
[d] $CD4^-CD8^+$	7.1 ± 0.4	-	6.4 ± 0.2	-	6.1 ± 0.5	-	NS
[e] $NK1.1^+CD3^-$	2.3 ± 0.2	-	2.2 ± 0.2	-	1.9 ± 0.1	-	$p \leq 0.05$
[f] $MAC\text{-}3^+$	8.0 ± 0.3	-	8.2 ± 0.9	-	6.8 ± 0.4	-	$p \leq 0.05$
1 µm C60							
Mass-Based Exp. Conc. (mg/m^3)	*0*	*2*	-	*15*	-	*30*	-
Spleen Cells ($\times 10^6$)	147.7 ± 7.0	151.2 ± 10.4	-	147.5 ± 6.5	-	150.0 ± 7.5	NS
[a] Ig^+	107.6 ± 4.8	100.6 ± 5.9	-	99.2 ± 5.0	-	101.9 ± 5.3	NS
[b] $CD3^+$	20.2 ± 1.4	18.7 ± 2.2	-	20.5 ± 1.7	-	19.6 ± 2.1	NS
[c] $CD4^+CD8^-$	13.6 ± 0.9	12.3 ± 1.9	-	13.5 ± 1.3	-	11.8 ± 1.3	NS
[d] $CD4^-CD8^+$	6.2 ± 0.3	5.4 ± 0.8	-	4.9 ± 0.5 ††	-	3.5 ± 0.4 ††	$p \leq 0.01$
[e] $NK1.1^+CD3^-$	1.9 ± 0.1	1.8 ± 0.1	-	2.2 ± 0.2	-	1.9 ± 0.2	NS
[f] $MAC\text{-}3^+$	7.2 ± 0.4	6.8 ± 0.2 †	-	5.9 ± 0.4 ††	-	5.6 ± 0.5 *††	$p \leq 0.01$
Percent Values							
50 nm C60							
Mass-Based Exp. Conc. (mg/m^3)	*0*	-	*0.5*	-	*2*	-	-
[a] Ig^+	65.1 ± 1.8	-	58.0 ± 3.2 ††	-	59.1 ± 2.0 ††	-	$p \leq 0.05$
[b] $CD3^+$	16.3 ± 1.0	-	14.1 ± 0.9	-	16.0 ± 0.8	-	NS

	Control	C60 Fullerene (m^2/m^3)					Trend Analysis
		0.011	**0.033**	**0.084**	**0.112**	**0.167**	
[c] $CD4^+CD8^-$	10.6 ± 0.6	-	9.7 ± 0.5	-	10.9 ± 0.6	-	NS
[d] $CD4^-CD8^+$	4.1 ± 0.3	-	4.0 ± 0.2	-	4.2 ± 0.3	-	NS
[e] $NK1.1^+CD3^-$	1.4 ± 0.1	-	1.4 ± 0.1	-	1.3 ± 0.1	-	NS
[f] $MAC\text{-}3^+$	4.6 ± 0.2	-	5.0 ± 0.5	-	4.7 ± 0.2	-	NS
1 μm C60							
Mass-Based Exp. Conc. (mg/m^3)	*0*	*2*	-	*15*	-	*30*	-
[a] Ig^+	72.9 ± 1.0	67.0 ± 2.3 *††	-	67.4 ± 2.5	-	68.1 ± 1.0 **††	p ≤ 0.05
[b] $CD3^+$	13.6 ± 0.5	12.2 ± 0.7 †	-	13.8 ± 0.6	-	12.9 ± 0.9	NS
[c] $CD4^+CD8^-$	9.1 ± 0.2	7.9 ± 0.8 †	-	9.1 ± 0.6	-	7.8 ± 0.6 †	NS
[d] $CD4^-CD8^+$	4.2 ± 0.1	3.5 ± 0.3	-	3.3 ± 0.3	-	2.4 ± 0.2 ** ††	p ≤ 0.01
[e] $NK1.1^+CD3^-$	1.3 ± 0.1	1.2 ± 0.1	-	1.5 ± 0.1	-	1.3 ± 0.1	NS
[f] $MAC\text{-}3^+$	4.9 ± 0.4	4.6 ± 0.3	-	4.0 ± 0.2	-	3.8 ± 0.3	p ≤ 0.01

Mass-Based Exp. Conc. = Mass-Based Exposure Concentration

Spleen cell subsets defined based strictly on the presence or absence of the surface markers tested:

[a] B-lymphocyte;

[b] T-lymphocyte;

[c] Helper T-lymphocyte;

[d] Cytotoxic T-lymphocyte;

[e] Natural Killer cell;

[f] Macrophage

Values represent the mean (± SE) from 8 animals per group;

* $p < 0.05$ and

** $p < 0.01$ from control (mass basis);

† $p < 0.05$ and

$\dagger\dagger$ $p < 0.01$ from combined controls (surface area basis; calculated via methods described in Sayers et al. 2016)

Combined control groups were used for surface area basis comparisons; see Supplementary Table S1 for combined control means

Table 4

Bronchoalveolar lavage (BAL) cell phenotypes in female Wistar Han rats following 13-week inhalation of C60

	Control	C60 Fullerene (m^2/m^3)					Trend Analysis
		0.011	0.033	0.084	0.112	0.167	
Absolute Values (× 10^4)							
50 nm C60							
Mass Exposure *Concentration (mg/m^3)*	*0*	-	*0.5*	-	*2*	-	-
BAL Cells	107.7 ± 7.1	-	103.0 ± 7.2	-	98.0 ± 6.5	-	NS
$CD163^-CD11b^-$	92.6 ± 6.5	-	95.8 ± 6.9	-	92.9 ± 7.8	-	NS
$CD163^+CD11b^-$	0.4 ± 0.1	-	0.5 ± 0.2	-	0.2 ± 0.1	-	NS
$CD163^-CD11b^+$	1.1 ± 0.3	-	4.8 ± 2.6	-	3.7 ± 2.1	-	NS
$CD163^+CD11b^+$	13.5 ± 3.8	-	1.9 ± 0.9 **††	-	1.2 ± 0.5 **††	-	$p \leq 0.01$
1 μm C60							
Mass Exposure Concentration (mg/m^3)	*0*	*2*	-	*15*	-	*30*	-
BAL Cells	101.8 ± 7.1	99.0 ± 8.5	-	97.8 ± 11.2	-	149.2 ± 19.2	$p \leq 0.05$
$CD163^-CD11b^-$	80.4 ± 7.9	97.5 ± 8.3	-	96.5 ± 10.9	-	137.2 ± 20.2	$p \leq 0.01$
$CD163^+CD11b^-$	0.5 ± 0.2	0.1 ± 0.1	-	0.2 ± 0.1	-	0.3 ± 0.1	NS
$CD163^-CD11b^+$	1.6 ± 0.5	1.0 ± 0.5	-	0.7 ± 0.2	-	10.6 ± 2.8 **††	$p \leq 0.01$
$CD163^+CD11b^+$	19.4 ± 8.7	0.4 ± 0.1 **††	-	0.3 ± 0.1 **††	-	1.1 ± 0.3 **††	$p \leq 0.05$
Percent Values							
50 nm C60							
Mass Exposure Concentration (mg/m^3)	*0*	-	*0.5*	-	*2*	-	-
$CD163^-CD11b^-$	86.2 ± 3.4	-	93.3 ± 3.0 †	-	94.1 ± 3.4 †	-	$p \leq 0.05$
$CD163^+CD11b^-$	0.4 ± 0.1	-	0.5 ± 0.2	-	0.2 ± 0.1	-	NS
$CD163^-CD11b^+$	1.1 ± 0.3	-	4.4 ± 2.1	-	4.4 ± 2.8	-	NS
$CD163^+CD11b^+$	12.4 ± 3.1	-	1.8 ± 0.8 **††	-	1.3 ± 0.6 **††	-	$p \leq 0.01$
1 μm C60							
Mass Exposure Concentration (mg/m^3)	*0*	*2*	-	*15*	-	*30*	-
$CD163^-CD11b^-$	80.9 ± 7.6	98.5 ± 0.5 **††	-	98.8 ± 0.3 **††	-	90.5 ± 2.9	NS

	Control	C60 Fullerene (m^2/m^3)					Trend Analysis
		0.011	**0.033**	**0.084**	**0.112**	**0.167**	
$CD163^+CD11b^-$	0.4 ± 0.2	0.1 ± 0.1	-	0.2 ± 0.1	-	0.2 ± 0.1	NS
$CD163^-CD11b^+$	1.4 ± 0.4	1.0 ± 0.5	-	0.7 ± 0.2	-	8.4 ± 2.5 ** ††	$p \leq 0.05$
$CD163^+CD11b^+$	17.3 ± 7.1	0.4 ± 0.1 ** ††	-	0.3 ± 0.1 ** ††	-	0.9 ± 0.3 ** ††	$p \leq 0.01$

Mass-Based Exp. Conc. = Mass-Based Exposure Concentration

BAL cell subsets defined based strictly on the presence or absence of the two surface markers tested

Values represent the mean (± SE) from 8 animals per group;

** $p < 0.01$ from control (mass basis);

† $p < 0.05$ and

†† $p < 0.01$ from combined controls (surface area basis; calculated via methods described in Sayers et al. 2016)

See Supplementary Table S1 for combined control means.

NS = Not Significant